XVIII International Conference on "MATERIAL HANDLING, CONSTRUCTIONS AND LOGISTICS"

ANALYTIC AND EXPERIMENTAL INVESTIGATIONS ON A RESCUE DEVICE

Georg Kartnig[1], Christian Landschützer[2]

[1]TUG - Graz University of Technology, Institute of Material Handling and Logistic Systems
Inffeldgasse 25E, A-8010 Graz, Austria, email: kartnig@mhi.tugraz.at
[2] TUG - Graz University of Technology, Institute of Material Handling and Logistic Systems
Inffeldgasse 25E, A-8010 Graz, Austria, email: landschuetzer@mhi.tugraz.at

Abstract: *Rescue devices for roping down persons from a great height are usually based on the fly-wheel brake principle. The problem with these devices is, that they are worn out relatively quickly due to strong overheating (up to 800°C) and that their characteristics – for example the descend speed – are changed subsequently. In this paper we show, how these changes on a rescue device are recorded experimentally and derived by analytical and simulation methods. Also it shows how the parameters of the rescue device relevant for its using characteristics were optimized so far, that the device in his series version is in accordance with the intended standard.*

Keywords: *Rescue device, fly-wheel brake, multi body dynamics, simulation*

1. INTRODUCTION – DESCRIPTION OF THE RESCUE DEVICE

Rescue devices are produced, so that people can rope down out of dangerous situations (e.g. out of burning sky scrapers) and in this way bring themselves in safety. Beside professional rescue devices, as used by fire men, military personal, cableway companies and the police, there has been a tendency in the past few years to make models for private users.

Our Institute (Institute of Material Handling and Logistic Systems) received such a rescue device for investigation and improvement, so that it could stand an intended standard examination (DIN EN341 [2]) positively.

Like most rescue devices this one is also based upon the fly-wheel brake principle. It contains two fly-wheel brakes of the simplex-drum brake type [1]. The two drum brakes are synchronized with gears. With one of the gears there is a rope wheel rigidly connected. A rope is placed around this rope wheel, on which rescue overalls can be fixed on each end with the help of carabiners (Figure 1).

For the roping down process the rescue device is attached to a window frame or to the ceiling above of the balcony. The person wanting to rope down, puts on a rescue overall, then fixes it to one end of the rope and abseils along the wall of the building. Arriving on the ground floor, he takes off the rescue overall. Now the other end of the rope is situated at the level the first person fled from. So that a second person with a rescue overall can now escape in the same manner. In this way several persons can be saved quickly in a pendulum manner out of an altitude up to 300 m.

The most important characteristic of these rescue devices is their reliability under any imaginable conditions.

A standard defines the specifications and test processes for rescue devices: DIN EN341 [2]. Amongst other parameters this standard defines the descending speed for descending persons weighing 30 kg, 75 kg and 150 kg as being between 0.5 m/s and 2.0 m/s.

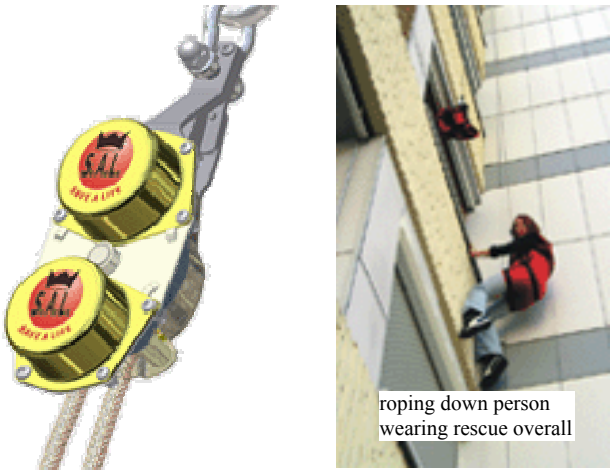

Figure 1. Rescue device

Following this standard, experimental tests at the Institute of Material Handling and Logistic Systems were carried out. Additionally the temperature of the drum brakes was investigated, so as to be able to make a clear statement about the durability of the brake linings used.

To reach a deeper understanding about the function of the rescue device, the inter-relationship between descend speed, descend weight and friction coefficient

of the brake linings is investigated by calculation in the following chapter.

2. STATIC CALCULATION

As mentioned above, the function of the rescue device is based upon the principle of fly-wheel brakes. Figure 2 shows the construction of the drum brake and figure 3 the calculation model with the acting forces, that build the basis for the calculation.

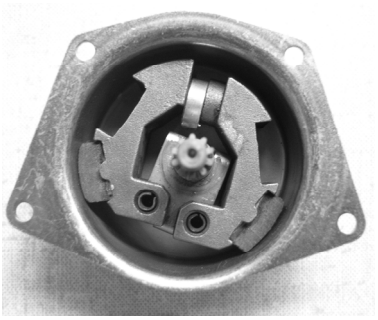

Figure 2. Fly-wheel brake

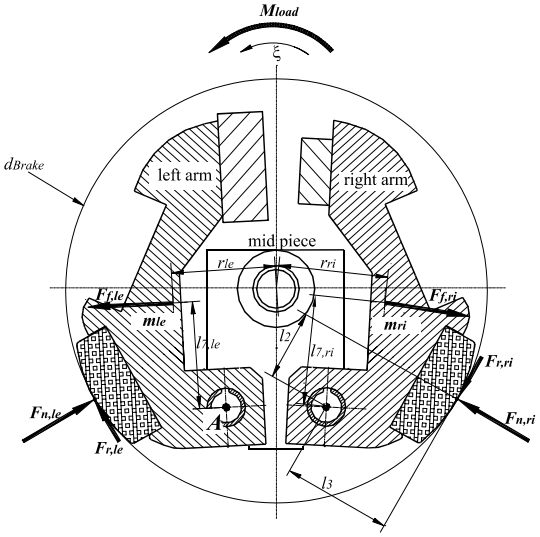

Figure 3. Forces on the fly-wheel brake (static model)

The centrifugal force on the left, pulled brake arm is:

$$F_{f,le} = m_{le} r_{le} \dot{\xi}^2 \tag{1}$$

Here is m_{le} the mass of the left brake arm, r_{le} the distance between rotation axis and the centre of gravity of the brake arm and $\dot{\xi}$ the angular velocity of the rotating brake.

Out of the momentum equilibrium around point A, one derives for the left brake arm (with l_2 and l_3 equal for left and right brake arm):

$$F_{f,le} l_{7,le} - F_{r,le} l_3 - F_{n,le} l_2 = 0 \tag{2}$$

With

$$F_{r,le} = \mu F_{n,le} \tag{3}$$

the friction force $F_{r,le}$ for the pulled brake arm can be derived following the simple Coulomb friction model:

$$F_{r,le} = \frac{\mu F_{f,le} l_{7,le}}{\mu l_3 + l_2} \tag{4}$$

For the other – the pushed – brake arm the sign of the denominator must be inverted. So $F_{r,ri}$ becomes:

$$F_{r,ri} = \frac{\mu F_{f,ri} l_{7,ri}}{-\mu l_3 + l_2} \tag{5}$$

and the brake force F_{Brake} of one drum brake becomes:

$$F_{Brake} = F_{r,le} + F_{r,ri} \tag{6}$$

As our rescue device consists of two drum brakes, the complete brake force $F_{Brake,tot}$ is:

$$F_{Brake,tot} = 2 F_{Brake} \tag{7}$$

and the total brake momentum:

$$M_{Brake,tot} = F_{Brake,tot} \frac{d_{Brake}}{2} i_{Gear} \tag{8}$$

with d_{Brake} as the inner diameter of the drum brake and i_{Gear} as the gear ratio between the rotating brake arms and the rope wheel.

This total brake momentum $M_{Brake,tot}$ is equal to the pulling force on the rope of the rescue device (= weight force of a descending person) multiplied with the effective radius of the rope wheel $r_{rope\text{-}wheel}$:

$$M_{Brake,tot} = m_{Person} g r_{rope-wheel} \tag{9}$$

This way the angular velocity of the rotating brake arms $\dot{\xi}$ can be calculated for the stationary operation.

$$\dot{\xi} = \sqrt{\frac{m_{Person} g \frac{d_{Rope}}{2} i_{Gear}}{d_{Brake} \mu \left(\frac{m_{le} r_{le} l_{7,le}}{\mu l_3 + l_2} + \frac{m_{ri} r_{ri} l_{7,ri}}{-\mu l_3 + l_2} \right)}} \tag{10}$$

Furthermore the descend speed v_{rope} depending on the weight of the descending person and the friction coefficient μ can be derived.

$$v_{Rope} = \frac{\dot{\xi} r_{rope-wheel}}{i_{Gear}} \tag{11}$$

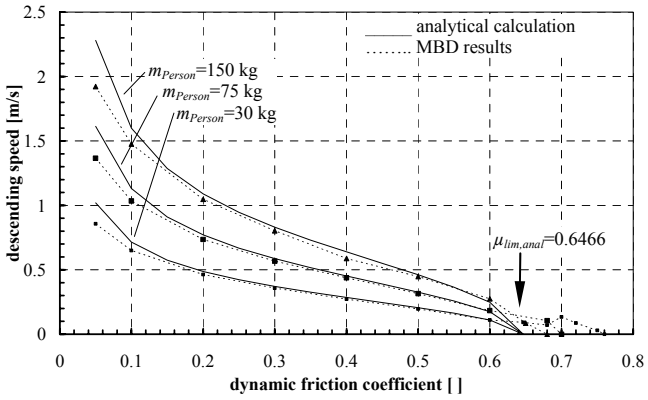

Figure 4. Descend speed

Figure 4 shows the descend speed. One can see, that – with a given weight of the brake arms – the friction coefficient μ must be between 0.07 and 0.2, so that the descend speed of 30 kg, 75 kg and 150 kg lies within the prescribed range of between 0.5 m/s and 2 m/s. Furthermore one can see, that the rescue device blocks at a friction coefficient $\mu_{lim,anal}$>0.6466.

3. DYNAMIC MODELLING

As the static calculation does not consider variable forces and the changing geometry caused by rotation it can not describe the system completely. Furthermore the descending person is hanging on a vibratory visco-elastic rope. The following section goes on to describe all these phenomena.

All of the results are calculated with μ=0.41 given from brake linings manufacturer and 75 kg person.

3.1 Dynamic behaviour of fly wheel brakes

For the dynamic modelling there are some more forces involved than for the static calculation. Mainly inertia forces and the weight affect dynamic relations with dependence on rotation angle ξ.

Figure 5 shows all geometric relations and all acting forces. With m_{le} and m_{ri}, the masses oft the left and right brake arms and m_2 mass of the mid piece and J, J_2 the moments of inertia all dynamic forces and magnet's force depending on the distance to one another are described in table 1 and 2.

Table 1. Dynamic forces on brake arms

left arm with magnet *(right arm equals with index ri)*	
$\vec{F}_{f,le} = m_{le} r_{le} (\dot{\vec{\xi}})^2$	centrifugal force
$\vec{F}_{n,le} = \vec{s}_{le} c + \dot{\vec{s}}_{le} d$	normal force
$\vec{s}_{le} = l_{2,le} \vec{\varphi}_{le}$	penetration
$\vec{F}_{n,le} = l_{2,le} (\vec{\varphi}_{le} c + \dot{\vec{\varphi}}_{le} d)$	normal force with $-l_{2,ri}$ for right arm
$\vec{F}_{r,le} = \mu \vec{F}_{n,le}$	friction force
$\vec{F}_{T,le} = m_{le} l_{4,le} \ddot{\vec{\varphi}}_{le}$	force fr. rotating inertia
$\vec{F}_{D,le} = m_{le} (\ddot{\vec{x}} + \ddot{\vec{y}})$	force fr. transl. inertia
$\vec{F}_{Gm,le} = m_{le} \vec{g}$	weight
$\vec{F}_{mag,le} = \vec{F}_{mag,ri} = \vec{F}_{mag} = \begin{vmatrix} 2\text{N} & \lvert\vec{a}\rvert \le a_{min} + 0.1\text{mm} \\ 0 & \lvert\vec{a}\rvert > a_{min} + 0.1\text{mm} \end{vmatrix}$	magnet force

For the magnet force the distance between the two brake arms has to be calculated (neglecting small angles for trigonometry):

$$\vec{a} = l_6 \vec{\varphi}_{le} - l_6 \vec{\varphi}_{ri} \qquad (12)$$

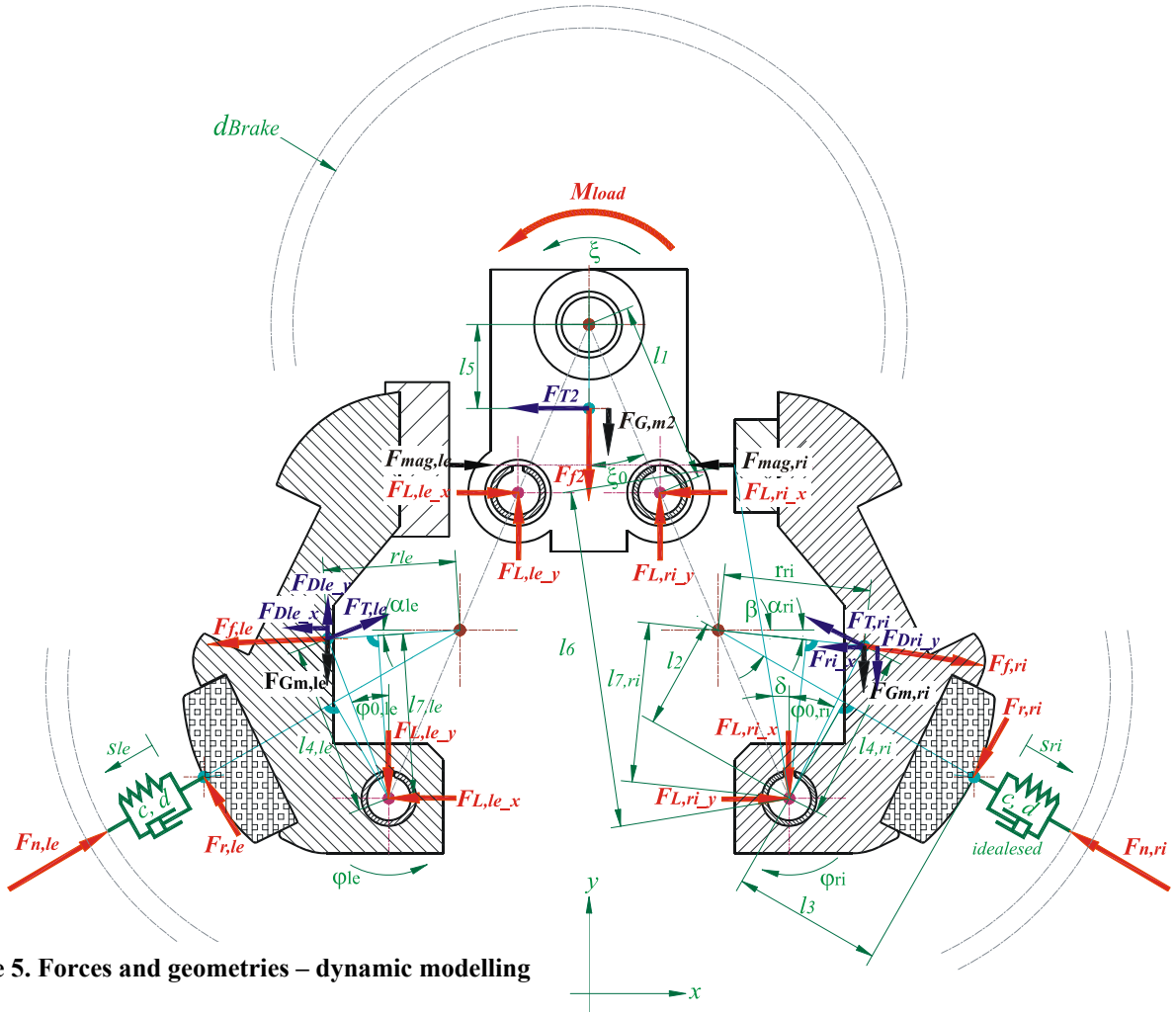

Figure 5. Forces and geometries – dynamic modelling

Table 2. Dynamic forces on mid piece

mid piece names s. Table 1.
$\vec{F}_{f2} = m_2 l_5 (\dot{\vec{\xi}})^2$
$\vec{F}_{T2} = m_2 l_5 \ddot{\vec{\xi}}$
$\vec{F}_{D2} = m_2 (\ddot{\vec{x}} + \ddot{\vec{y}})$
$\vec{F}_{Gm2} = m_2 \vec{g}$

To determine the friction force the dynamic friction coefficient is needed. This coefficient is modelled depending on stiction and transition velocities especially for small velocities. With this approach non-continuous functions are eliminated.

Now using tables 1 and 2 nine differential equations – principles of linear and conservation of angular momentum – can be derived to solve for all nine unknown terms listed below (with bolt reaction force labelled F_L):

$$\varphi_{le}, \varphi_{ri}, \xi, x, y, F_{L,le\_x}, F_{L,le\_y}, F_{L,ri\_x}, F_{L,ri\_y}$$

Components *'x'* and *'y'* of all forces consider the rotating ξ-system and are not fully described here e.g.

$$\vec{F}_{f,ri\_x} = \left|\vec{F}_{f,ri}\right| \cos(\xi - \alpha_{ri}) = F_{f,ri\_x} \qquad (13)$$

left arm:

$$m_{le}\ddot{x} + F_{T,le\_x} + F_{n,le\_x} - F_{r,le\_x} - F_{L,le\_x} - F_{f,le\_x} + F_{mag,le\_x} = 0 \qquad (14)$$

$$m_{li}\ddot{y} + F_{T,le\_y} + F_{n,le\_y} + F_{r,le\_y} - F_{L,le\_y} - F_{f,le\_y} - F_{Gm,le\_y} + F_{mag,le\_y} = 0 \qquad (15)$$

$$-J_{le}\ddot{\varphi}_{le} - F_{n,le}l_{2,le} - F_{r,le}l_{3,le} + F_{f,le}l_{7,le} + F_{G,mle}l_{4,le}\sin(\xi + \varphi_{0,le}) + F_{mag}l_6\cos\delta + F_{D,le\_x}l_{4,le}\cos(\xi + \varphi_{0,le}) - F_{D,le\_y}l_{4,le}\sin(\xi + \varphi_{0,le}) = 0 \qquad (16)$$

right arm:

$$-m_{ri}\ddot{x} - F_{T,ri\_x} - F_{n,ri\_x} - F_{r,ri\_x} + F_{L,ri\_x} + F_{f,ri\_x} - F_{mag,ri\_x} = 0 \qquad (17)$$

$$m_{ri}\ddot{y} + F_{T,ri\_y} + F_{n,ri\_y} - F_{r,ri\_y} - F_{L,ri\_y} - F_{f,ri\_y} - F_{Gm,ri\_y} - F_{mag,ri\_y} = 0 \qquad (18)$$

$$-J_{ri}\ddot{\varphi}_{ri} - F_{n,ri}l_{2,ri} - F_{r,ri}l_{3,ri} + F_{f,ri}l_{7,ri} + F_{G,mri}l_{4,ri}\sin(\xi - \varphi_{0,ri}) - F_{mag}l_6\cos\delta - F_{D,ri\_x}l_{4,ri}\cos(\xi - \varphi_{0,ri}) + F_{D,ri\_y}l_{4,ri}\sin(\xi - \varphi_{0,ri}) = 0 \qquad (19)$$

mid piece:

$$-m_2\ddot{x} + F_{f2\_x} - F_{T2\_x} + F_{L,le\_x} - F_{L,ri\_x} = 0 \qquad (20)$$

$$-m_2\ddot{y} - F_{f2\_y} - F_{T2\_y} + F_{L,le\_y} + F_{L,ri\_y} - F_{Gm2\_y} = 0 \qquad (21)$$

$$-J_2\ddot{\xi} + F_{L,le\_x}l_1\cos(\xi - \xi_0) + F_{L,le\_y}l_1\sin(\xi - \xi_0) - F_{L,ri\_x}l_1\cos(\xi + \xi_0) + F_{L,ri\_y}l_1\sin(\xi + \xi_0) + F_{Gm2}l_5\sin\xi - F_{D2\_x}l_5\cos\xi - F_{D2\_y}l_5\sin\xi + M_{load} = 0 \qquad (22)$$

There are different ways to solve a system of differential equations such as (14)-(22). First of all systems like these can only be solved numerically. The two most common possibilities are signal-flow oriented modelling (e.g. MATLAB-Simulink) and multi-body-dynamics (MBD). With MBD the compilation of differential equations by the user is not necessary for standard problems.

Although the equations are written down here, a MBD-solution was finally chosen for the analysis for several reasons. The MBD-method is less error-prone in the modelling process than signal-oriented modelling (e.g. problems with algebraic signs and solver settings) because it does not need user set up equations. Furthermore MBD can use real 3D solid geometry – imported from CAD – for contact calculation of new and worn brakes. Also MBD is – for the current problem – more accurate than solving (14)-(22) with signal-oriented systems because all these equations contain some simplifications especially for trigonometric functions. But one of the most attractive features of MBD is the possibility of visualisation in various ways.

Despite all of MBD's advantages the knowledge of the prescribing equations for the signal-oriented method is essential. Interpreting MBD results and influences of single phenomena as for example the weight of the brake arms (22) then becomes more transparent.

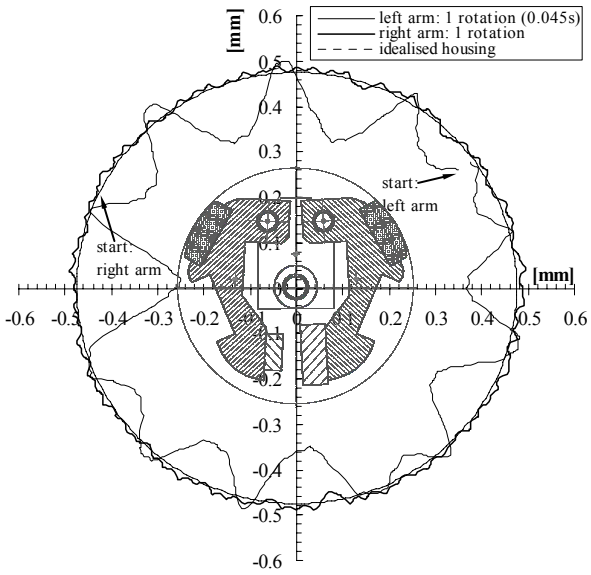

Figure 6. Penetration of brake drum during one rotation of left pulled and right pushed brake arm reduced to relative amplitudes with idealised housing radius equal 0.48 mm

One rotation of one of the two fly-wheel brakes with 75 kg applied person-mass and μ=0.41 needs 0.045 s and results in two main frequencies of the two arms penetrating the brake drum (Figure 6). The brake arms follow oscillating movement in there φ–systems, penetrate the brake drum and are reflected according to the contact stiffness c (Figure 5). During this penetration, friction force comes into affect thus decreasing the rotation speed. With a smaller rotation speed the centrifugal force decreases and thus the penetration ends. Now rotation speed increases and the penetration – with increasing centrifugal force – starts again.

Figure 6 shows two main frequencies for the arm oscillation φ_{le} and φ_{ri}. There are ~1770 Hz for the right – pushed arm and ~270 Hz for the left pulled arm. Both frequencies are very high and will not cause resonant vibrations in combination with the non-stiff rope (s. 3.2).

Changing the mass of the person and analysing descending speed versus time results in figure 7.

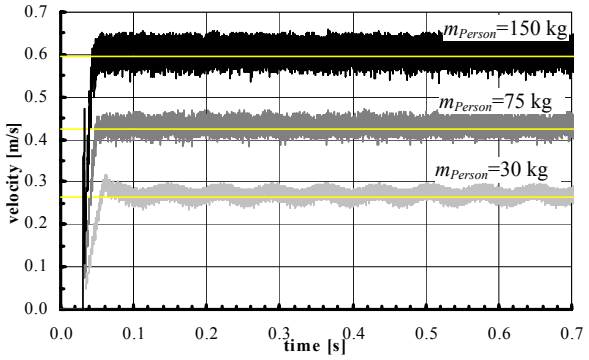

Figure 7. Descending speed (time dependend and middle) for different person masses

Because of the brake arm oscillations and their movement as described above, rotation speed is not constant and varying with the mentioned frequencies.

For the 30 kg person there is also influence from the gravity force as derived in (22) visible in the momentum-term $F_{Gm2}l_5\sin\xi$. This is the lowest relevant system frequency which has to be investigated in combination with the rope-person – system.

3.2 Dynamic behaviour of the rescue device with rope

For the complete model with roping down person a combination of both modelling methods (signal-flow oriented and MBD) is necessary to describe the elastic-damping rope with decreasing stiffness. Therefore user written differential equations can be implemented in MBD systems (Figure 9 and (25)-(26)) combining MBD with signal-flow oriented modelling.

Modelling the abseiling person, hanging on the visco-elastic rope – with the classic one-degree of freedom approach for forced damped vibrations – brings the connection between M_{load} (22) and following (14)-(21), ξ and the descending person with her vertical coordinate y_{person}. Rope length comes from:

$$l(\xi) = l = r_{rope-wheel}\xi \quad \text{and} \quad \dot{l} = r_{rope-wheel}\dot{\xi} \tag{23}$$

Neglecting all additional forces from wind and friction there is:

$$M_{load} = r_{rope-wheel}F_{rope} \tag{24}$$

with y_{person}:

$$F_{rope}(l) = c_{rope}(l)(l - y_{person}) + b_{rope}(l)(\dot{l} - \dot{y}_{person}) \tag{25}$$

describing dynamic movement of person with:

$$m_{person}\ddot{y}_{person} = F_{rope}(l) - m_{person}g \tag{26}$$

The rope (described in EN 1891 [3]) is made of low stretch kernmantel type. Various measurements of the vibratory personmass-rope-system were made and this showing that there are two main effective visco-elastic parameters involved: damping and stiffness. With $c_{spec,rope}$ [N] specific stiffness of 1m rope and $\Delta l(l_0)$ static elongation of l_0 long rope stiffness of the rope follows:

$$c_{rope}(l) = \frac{c_{spec,rope}}{l} \quad \text{and} \quad \Delta l(l_0) = \frac{m_{person}\cdot g}{c_{rope}(l_0)} \tag{27}$$

Damping is more complex and beside that experiments showed a strain dependent damping (following 'Reid-model') the Kelvin-Voigt model is used. This is adequate because only frequencies and maximum amplitudes are interesting [4]. Only observing material warming and creep needs more detailed damping modelling. Implementing length dependency in Lehr's attenuation factor with constant and length proportional terms brings the damping of the rope [5]:

$$b_{rope}(l) = 2\left(\frac{D_p}{l} + D_c\right)\sqrt{c_{rope}(l)m_{person}} \tag{28}$$

Using (27)-(28) the damped eigenfrequency (nearly equals eigenfrequency for low damping) of the one-mass oscillating system with l [m] rope is:

$$f(l) = \frac{1}{2\pi}\sqrt{\frac{c_{rope}(l)}{m_{person}} - \left(\frac{b_{rope}(l)}{2m_{person}}\right)^2} \tag{29}$$

Examining the lowest exciting frequency from rotation under gravity (22) brings one excitation per revolution:

$$f_{exc}^{(1)} = \frac{\dot{y}i_{Gear}}{2\pi r_{rope-wheel}} = \frac{\dot{\xi}}{2\pi} \tag{30}$$

Instead of calculating the resonant rope length $l^{(1)}$ analytically, a graphic solution is more transparent. $l^{(1)}$ then comes from the intersection of the exciting- and the eigenfrequency-curves. Figure 8 shows the intersection beyond 0.1 m rope length only. This rope length is two short for effects in real use, because the rescue device is always mounted overhead.

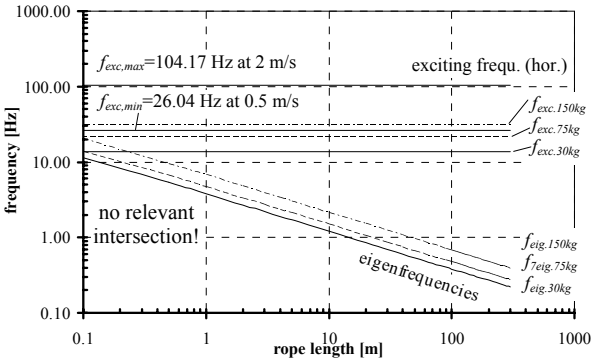

Figure 8. Eigen and lowest exciting frequencies at different masses

Higher resonances (270 Hz and 1770 Hz from 3.1) naturally drop out from calculation because of the very low eigenfrequencies of the soft rope-person system.

A complete dynamic solution of the descending person hanging on the rescue device is shown in figure 9.

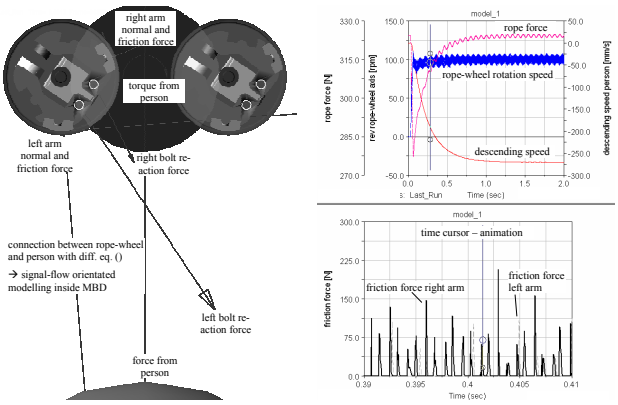

Figure 9. MBD solution (screenshot PostProcessor) of descending 30kg person

The main forces, such as rope force, bolt force F_L and friction-normal force are plotted exemplarily. The charts on the right show time based results.

Rope force decreases during brake acceleration because of the unloading of the pre-tensioned rope. Afterwards the rope force follows the excitation in non resonant stage.

Descending speed increases (y and time derivative negative!) and reaches a nearly oscillation free stage because of small rope force amplitudes and high damping.

Rotational speed of rope-wheel reaches nominal speed very soon; hanging person is following according to oscillation dynamics.

Friction force appears in short impulses as assumed in 3.1. According to figure 4 descending speed is not the same for equal acting forces (static calculation) and impulsive acting forces (dynamic solution). Also the different μ_{lim}'s at blocking stage can be explained from brake arm oscillation – and therefore impulsive acting friction forces – as well as from stick-slip processes. Penetration s from figure 5 lies within 0.4mm including the deformation of the brake drum.

Various parameter changes for contact stiffness c (figure 5) and additional friction in bearings do not show other results for interesting descend speed and rope force.

4. EXPERIMENTAL INVESTIGATIONS

To measure the real descend speed as well as the abrasion in real use and to validate static and dynamic models, the rescue device was investigated experimentally. For this purpose a test stand was built at the Institute of Material Handling and Logistic Systems. It consists of a stiff frame made of aluminium profiles and plates. On one of these plates, the rescue device is fixed (Figure 10).

In the rescue device the rope wheel was replaced by a chain wheel, so that the roping down force could be induced by a chain drive. The needed torque is applied by a torque controlled servo drive with a flange mounted planet gearbox. With a ratio of the planet gearbox of i_{planet}=10 and a ratio of the chain drive of i_{chain}=19/32 the descend weight of 75 kg at a rope wheel radius of 27.5 mm corresponds to a drive torque of 3.41 Nm.

Additionally the test stand contains a rotary encoder to measure the descend speed and a torque measuring device to control the torque of the servo drive. Furthermore a contactless working temperature measuring device was fixed on a tripod. All the measuring data were recorded with the help of the measuring software LABVIEW.

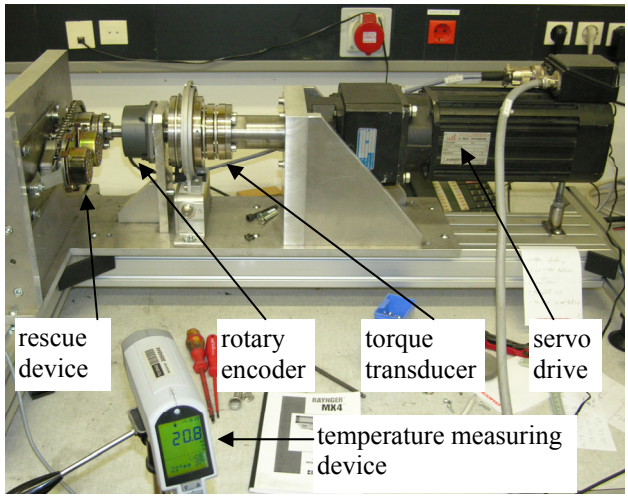

Figure 10. Rescue device test stand

During the measurements the following data were recorded:

- The speed of the chain wheel
- The drive torque
- The temperature of the drum brake

The measuring process was essentially equivalent to the DIN EN 341 [2] with the only difference, that the rescue device was tested for a descend height of 300m because of the assumed use for sky scrapers.

DIN EN 341 prescribes only a descend height of 100 m. So one test cycle consists of the following parts:

The rescue device is loaded with a torque corresponding to a descend weight of 75 kg. The descend height is 300 m, afterwards there is a break of 90 s. The next part of the test – also with a descend weight of 75 kg – goes the other way round. All in all there are seven tests with a descend weight of 75 kg. After that there is one test with a descend weight of 150 kg and at the end one test with a descend weight of 30 kg.

In the first test cycle the rescue device was supplied with brake linings with a maximum temperature of 250°C. The real temperatures were around 400°C, measured already during the first test after 3 minutes. The test had to be stopped, after one magnet came off and blocked the drum brake. The investigation of the rescue device afterwards showed, that the brake linings had burnt through completely.

As of the second test cycle the rescue devices were supplied with brake linings with a maximum temperature of 450°C. This time all seven tests with a descend weight of 75 kg could be carried out. Only during the eighth test with a descend weight of 150 kg did the rescue device fail: because of the very high temperatures (up to 800°C) the gears broke. During the measurement there could be seen, that the two drum brakes heated very differently. That means that the brake momentum of the two drum brakes was also very different. The reason being the different weights of the brake arms:

Brake 1:	Brake arm left:	47.5 g
	Brake arm right:	48.7 g
Brake 2:	Brake arm left:	50.0 g
	Brake arm right:	47.5 g

To get a symmetrical distribution of the brake momentum, the brake arms were milled and this way all four brake arms got the same weight of 47.5 g. As a consequence the third test cycle showed a much more symmetrical heating of the drum brakes.

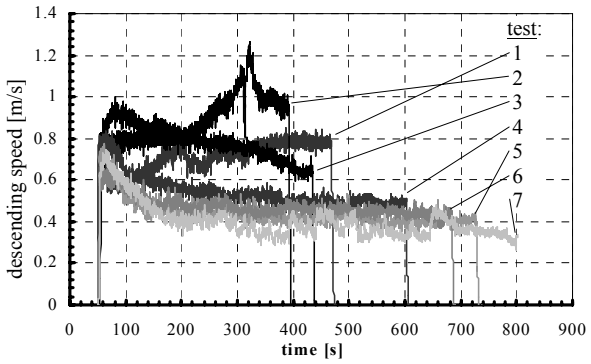

Figure 11. Results of the third test cycle

In Figure 11 one can see seven measuring curves, that show the descend speed with a descend weight of 75 kg. The descend speeds lie between ~0.35 m/s and ~1.2 m/s, whereas the first descend processes show higher and the later ones show slower speeds.

Furthermore you see, that the speed curves show a considerable noise. The reason for that could be found in multi body simulation. (see chapter 3).

The related temperature curve to this test cycle is shown in figure 7. One sees that from the second test on the temperatures become lower and the descend times become longer. That means: the heating of the drum brake causes an increase to the friction coefficient of the brake linings, the higher friction coefficient causes lower descend speeds and the lower descend speed means a lower break power and so a lower heating.

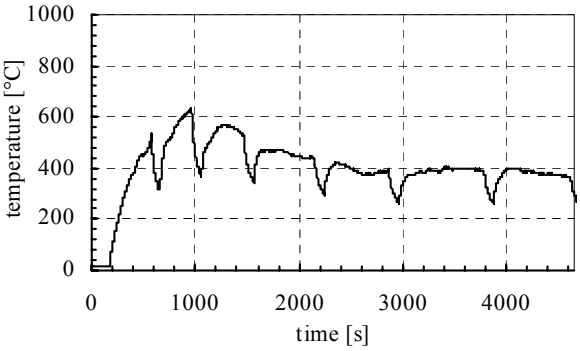

Figure 12. Temperature of one fly-wheel brake

But the most important statement about the measurements concerns the friction coefficient of the brake linings. With the measured descend speeds of figure 11 and with the help of (10) and (11) the related friction coefficients can be calculated. They lie between 0.15 and 0.48 (μ_{min} and μ_{max} – figure 13). This results – with the given brake arm weight of 47.5 g ($m_{current\ stage}$) – in calculated descend speeds of 0.25 m/s for a descend weight of 30 kg, μ=0.48 and 1.46 m/s for a descend weight of 150 kg, μ=0.15. That means the rescue device is too slow. The minimum of the measured speed remains under the minimal prescribed Standard descend speed, whereas the maximal prescribed Standard descend speed is not matched.

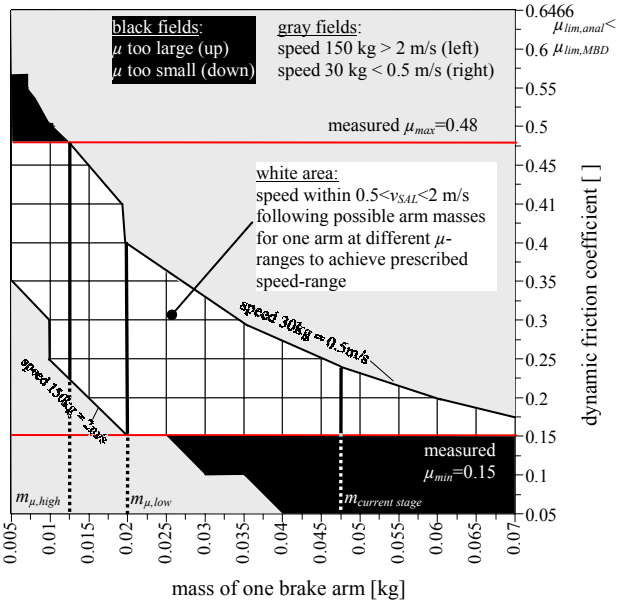

Figure 13. Connection between mass of one brake arm, dynamic friction coefficient and descend speed (field colour and limiting curves 0.5 and 2 m/s)

To remain – with the measured friction coefficient – within the prescribed speed range of 0.5 m/s to 2.0 m/s, the mass of the brake arms has to be reduced. With

equation (10) and (11) the connection between mass of the brake arms, friction coefficient and descend speed can be calculated (Figure 8). In this diagram you can see that a reduction of the weight of the brake arms is necessary so that the weight of each brake arm lies between 12.5 g and 20 g ($m_{\mu,high}$ and $m_{\mu,low}$). Even with these brake arm weights it is not possible to remain completely within the prescribed speed range. Either the rescue device is too fast ($m_{\mu,high}$, 150 kg and μ_{min}) or it is too slow ($m_{\mu,low}$, 30 kg and μ_{max}).

We recommend the highest possible weight of 20 g, because this way it is guaranteed, that the maximum speed is not above 2 m/s but can be below 0.5 m/s. This lower speed will occur to 30 kg persons (children) descending. Therefore it is intended to support the descending process by applying additional hand force on the tight side rope by person observing the rescue process of children.

With this brake arm weight, the problems concerning the brake arm design and heating can be minimalized.

5. CONCLUSION

In this paper we describe the investigation of a rescue device in three different ways: In the static calculation the connection between descend weight, friction coefficient of the brake linings and descend speed was shown. With the help of the multi body simulation we found out the reason for the noise in the descend speed and we could show, that there are no critical situations because of resonance. And in the experimental investigation we could show, that the real friction coefficients vary in a broad area and that small differences in the weight of the brake arms cause big differences to the load of the two drum brakes.

Based on this knwledge the rescue device was modified in the following points:

- The brake linings were changed
- The weight of the brake arms was equalized (all brake arms 47.5g)
- The weight of the brake arms was reduced in the simulation, so that the descend speed remained within the prescribed range for all descend weights

The final step – the reduction of the brake arms weight – needs a complete redesign of the arms and is therefore not realized yet. Experimental investigations of the efficiency of this step as well as investigations of the consequences concerning the heating of the drum brakes are planned for next time.

6. ACKNOWLEDGMENT

The authors would like to thank MARK GmbH & CoKG for the support with machine parts of the rescue device as well as valuable hints concerning problems that occurred in former tests.

7. REFERENCES

[1] Kurth, F., Scheffler, M.: *Grundlagen der Fördertechnik (Fundamentals of mechanical conveying)*, VEB Verlag Technik Berlin, 1976.

[2] DIN EN 341 *Persönliche Schutzausrüstung gegen Absturz – Abseilgeräte zum Retten (Personal protective equipment against falls from a height – Descender devices for rescue)*, 2003.

[3] EN 1891: *Kernmantelseile mit geringer Dehnung (Low stretch kernmantel ropes)*, 1998.

[4] Dresig, H.: *Schwingungen mechanischer Antriebssysteme* (*Oscillations of mechanical drives)*, Springer, Berlin, 2001.

[5] Landschuetzer, C.: *Analyse von Schwingungen an einsträngigen Elektrokettenzügen* (*Polygon effect induced oscillations of electro chain hoists*), Dissertation TU-Graz, Graz, 2004.